

Organic-Inorganic Hybrid Materials. 1. Hydrolysis and Condensation Mechanisms Involved in Alkoxysilane-Terminated Macromonomers

Françoise Surivet,[†] Thanh My Lam,^{*,‡} Jean-Pierre Pascault,[‡] and Quang Tho Pham[§]

Centre de Recherches Corning Europe, 7 bis avenue de Valvins, 77 211 Avon Cedex, France, Laboratoire des Matériaux Macromoléculaires, URA CNRS 507, Institut National des Sciences Appliquées de Lyon, 20, avenue Albert Einstein, 69 621 Villeurbanne Cedex, France, and CNRS, Service Central d'Analyses, BP 22-69 390 Vernaison, France

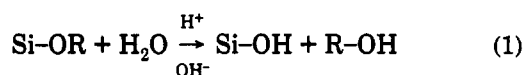
Received December 19, 1991; Revised Manuscript Received April 8, 1992

ABSTRACT: The hydrolysis and polycondensation reactions involving alkoxysilane groups have been studied in bulk using model compounds prepared from an isocyanate-functionalized prepolymer and (γ -aminopropyl)-triethoxysilane. The molecular weight evolution and the appearance of the different condensed species are followed by ^{29}Si NMR and size exclusion chromatography (SEC). Peak assignments of the ^{29}Si NMR experiments were determined by comparing two acid-catalyzed reactions. If hydrolysis is fast, the condensation reaction occurs at a upper rate at the first time and slower rate after. During the same reaction, the gel time is determined by dynamic mechanical measurements and by the appearance of insoluble fractions in different solvents. The scaling exponent for the variation of G' and G'' with frequency at the gel point is $\Delta = 0.63 \pm 0.02$, in agreement with the percolation theory. The extent of the reaction may be calculated from NMR and SEC results. The experimental conversion at gelation is found equal to 0.50, whereas the predicted value is 0.33. This difference can be explained by substitution effects and by intramolecular reactions.

Introduction

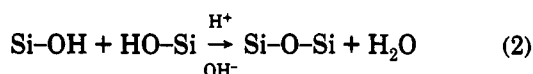
The hydrolysis and condensation reactions of alkoxy-silanes, specifically tetraethoxysilane and tetramethoxy-silane, lead to the formation of an oxide network, suggesting a possible way to form glass and ceramic materials. More recently, investigations on this kind of chemistry were focused on the use of silicon alkoxides and of alkoxysilane-terminated organic monomers or macromonomers M-Si(OR)_3 for different applications such as coupling agents for composites,^{1,2} coatings,³ electrolytes,⁴ or adhesives.⁵

Alkoxysilane groups react by way of a two-stage mechanism.^{6,7} The first stage is hydrolysis, which can be written as

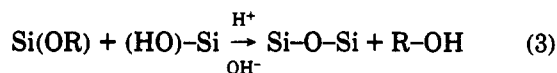


The second reaction is condensation, of which there are two kinds:

Water-producing condensation



Alcohol-producing condensation



Reactions of tetraalkoxysilanes or trialkoxysilane-terminated macromonomers are similar and give siloxane -Si-O-Si- bonds. These compounds can also be useful as models to study the chemistry and the polymeric parameters controlling the processing of such materials.

These reactions can occur in either basic or acidic mediums. The reaction conditions influence the relative

rates of the two-stage reactions and the chemistry of the sol-gel process. Different comparisons have been done in the literature between the acid- or base-catalyzed gels. It seems that the gel process is homogeneous in the case of an acid-catalyzed reaction and heterogeneous (colloidal) in the case of a base-catalyzed reaction. These two processes lead to a lightly cross-linked polymer in the first case and to densely cross-linked particles in the second case.⁷⁻¹⁰

The water concentration also affects the polymer structure and the gel formation.¹¹ The hydrolysis ratio and the nature of the catalyst are the most important parameters in the silicon tetraalkoxide sol-gel process. However, other parameters such as concentration,¹² nature of the solvent,¹³ and temperature¹⁴ can also play a decisive role in the kinetics and the choice of the reaction pathway.

Chemistry has to be related to the rheological changes occurring during the thermoset process. The hydrolysis and condensation of silane-terminated organic monomers or macromonomers lead to insoluble polymers and network formations. When a homogeneous thermoset system cures, two principal structural transitions may occur: gelation and vitrification. Gelation marks the transition from a liquid to a rubbery state, since the cross-linked network has elastic properties not present in the low-molecular-weight, linear or branched prepolymers. Vitrification involves a transition from the liquid or rubbery state into the glassy state as a consequence of an increase in molecular weight before gelation or an increase in cross-link density after gelation; more precisely, it involves a loss of free volume as molecular weight and cross-linking density increase. It is important to describe the gelation phenomenon from a technological and a theoretical point of view. There are two general classes of polymerization models that are applicable to the gelation of alkoxysilanes: the random branching network model¹⁵ and percolation simulations.¹⁶ A recent paper⁷ reviews the experimental evidence which suggests that the gelation of alkoxides can be modeled using analyses developed for organic condensation polymerization. The conversion at the gel point is

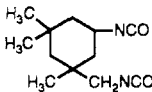
* To whom correspondence should be addressed.

[†] Centre de Recherches Corning Europe.

[‡] Laboratoire des Matériaux Macromoléculaires.

[§] CNRS.

Table I
Characteristics of the Different Monomers Used

| monomers | formulas | molecular weight | melting point (°C) | suppliers |
|--|---|------------------|--------------------|-----------|
| α -hydroxy- ω -methylpoly(ethylene oxide) (PEO1) | $\text{CH}_3(\text{OCH}_2\text{CH}_2)_n\text{OH}$ | 350 | -8 | Aldrich |
| α,ω -dihydroxypoly(ethylene oxide) (PEO2) | $\text{HO}(\text{CH}_2\text{OCH}_2)_n\text{OH}$ | 400 | 8 | Aldrich |
| isophorone diisocyanate (IPDI) |  | 222 | | Aldrich |
| (γ -aminopropyl)triethoxysilane (γ -APS) | $\text{NH}_2(\text{CH}_2)_3\text{Si}(\text{OC}_2\text{H}_5)_3$ | 221 | | Aldrich |
| (γ -aminopropyl)dimethylethoxysilane (γ -APDMES) | $\text{NH}_2(\text{CH}_2)_3\text{Si}(\text{CH}_3)_2(\text{OC}_2\text{H}_5)$ | 162 | | Petrarch |

especially well predicted using the recursive solution of random branching model assuming some ring formation or substitution effects.⁷

A substitution factor r has been introduced which modifies the reactivity of functional groups depending on how many of the functional groups have been condensed. The consequences of the substitution effect have been averaged into one factor. Generally, r is less than 1 meaning that the reactivity decreases with condensation. This r factor is an adjustable parameter in the recursive model. In the case of the tetraalkoxysilane monomer, for no ring formation or substitution effects ($r = 1$), i.e. the ideal assumptions of the Flory-Stockmayer model, the conversion at gelation, x_{gel} , is 1/3; but $x_{\text{gel}} = 0.412$ if $r = 0.5$ and $x_{\text{gel}} = 0.454$ if $r = 0.1$.

Cyclization can also modify the conversion at the gel point. If $r = 1$ and 36% of the condensation reactions that occur are intramolecular reactions, the maximum effective conversion would be 0.32 and the reactive liquid could never reach the critical conversion for gelation. If $r = 0.5$, then only 18% of the reactions needs to be ring forming to prevent the sol for gelling, and for $r = 0.1$, only 10% is needed to prevent gelation. So, for a given r value, the difference between the experimental conversion and the predicted gelation conversion, x_{gel} , can be explained by cyclization.⁷

The Flory-Stockmayer mean-field theory and percolation models both provide scaling relations for the divergence of static properties, such as the weight average molecular weight, \bar{M}_w , or the zero shear rate viscosity, η_0 , of the polymeric species at the gelation threshold. But from a general point of view, the mean-field theory correctly predicts the conversion at the gel point but percolation models can describe better the approach to the critical phenomena.¹⁶ Considerations of the dynamics near the critical gelation point have led to predictions for the frequency dependence of the complex shear modulus

$$G^*(\omega) = G'(\omega) + iG''(\omega)$$

where $G'(\omega)$ and $G''(\omega)$ are the storage and loss shear moduli, respectively. More precisely, at the gel point, G' and G'' are scaled with frequency as

$$G' \propto G'' \propto \omega^\Delta$$

The predicted values from percolation theory is $\Delta = 0.67$.¹⁷ Experimentally, the observed scaling at the gel point is $\Delta = 0.70 \pm 0.05$ for epoxy amino systems,¹⁸ 0.5–0.69 for polyurethanes depending on the authors^{19,20} and the stoichiometric ratio,²⁰ and 0.72 ± 0.02 for a tetraethoxysilane system catalyzed by an acid.²¹ If the percolation theory has been quite successful in predicting the static properties (such as the distributions of molar masses and sizes) of branched polymers near the gel point, the dynamics of each system prior the gel point are not completely understood at present. What is needed is a quasi "universal" theory which is capable of predicting the entire frequency dependence of viscoelastic response

for a particular system, taking into account the functionality, the stoichiometric ratio, the sol and gel compositions, and the growth of polymeric clusters (fractals). A general rheological definition of the gel point is written as

$$G''/G' = \tan(\Delta\pi/2)$$

Δ being the common exponent of the power laws at the gel point. This equation, as a consequence of power-law behavior, falls out directly from the decades old Kramer-Kronig formula.

For polyurethanes based on a diol and a polyfunctional isocyanate at stoichiometric conditions, the authors found $\Delta = 0.5$. Under nonstoichiometric conditions, especially when the amount of cross-linker is deficient, with respect to the stoichiometry, $\text{NCO}/\text{OH} < 1$, they found $\Delta = 2/3$. This evolution from $\Delta = 0.5$ to 0.67 is explained by two types of behaviors, Zimm-like and Rouse-like for the relaxation time of a macromolecule approaching infinite dimensions, depending on its environment and especially the number of discrete macromolecules at the gel point (when this number increases, Δ increases). Martin et al.,³⁹ in an approach based upon the self-similar connectivity of branched molecules and upon a scaling theory of fractal correlations, proposed that the exponent values limits are 0.67–1.

The aim of this work is to investigate the hydrolysis and condensation reactions of alkoxysilanes. For that we use two types of silane-terminated macromonomers: (i) a two-end silane-terminated macromonomer with an alkoxysilane functionality, $\bar{f}_w = 2$. (Hydrolysis and condensation reactions were investigated by size exclusion chromatography analysis. Two-end silane-terminated macromonomers with higher alkoxysilane functionality, $\bar{f}_w = 6$, will be also used in the aim to prepare networks); (ii) a preponderantly single-end silane-terminated macromonomer, the synthesis of which is described in a previous paper.²² (Alkoxysilane functionalities are $\bar{f}_n = 3.6$ and $\bar{f}_w = 4$. The advancement of the reaction was determined by ²⁹Si NMR spectroscopy and size exclusion chromatography. The gel time was observed by dynamic mechanical measurements and insoluble fraction measurements. In addition, the scaling at the gel point was measured.)

Experimental Section

Starting Reagents. The formulas, molecular weights, and suppliers of the different materials are listed in Table I. The various products were used as received. The monoalcohol and macrodiol were degassed at 60 °C for 48 h before use. The catalysts used are trifluoromethanesulfonic acid (triflic acid), $\text{CF}_3\text{SO}_3\text{H}$, and hydrochloric acid, HCl .

Characterization. The analyses of the soluble products were made on a Waters chromatograph equipped with a 6000A pump, U6K injector, double detector (UV at $\lambda = 254$ nm), and differential refractometer (R401). The eluants used were tetrahydrofuran (THF) or chloroform (CHCl_3), and the separation was carried out using four μ styragel columns ($10^5 \text{ \AA} + 10^4 \text{ \AA} + 10^3 \text{ \AA} + 5 \times 10^2 \text{ \AA}$) with an elution rate of 1.5 mL/min. The approximate average molecular weights (\bar{M}_n , \bar{M}_w) were calculated using a polystyrene calibration.

²⁹Si NMR spectra were taken with a Bruker AC 200 spectrometer at 39.7 MHz in deuteriochloroform CDCl₃ solvent and with tetramethylsilane (TMS) as the internal reference. A Rheometrics dynamical analyzer (RDA 700) was used for performing dynamic mechanical measurements. The reactive mixture was placed between the 25-mm-diameter parallel disks of the rheometer. At regular time intervals, the reactions were examined in the frequency sweep mode. The chosen temperature was 40 °C and was held constant. The strain amplitude was held constant at 1% for the entire study.

Macromonomer Synthesis. (i) α,ω silane-terminated macromonomers were prepared via a two-step reaction, which is resumed in Figure 1. A macrodiol (1 mol) was reacted with 2 mol of isophorone diisocyanate (IPDI) in order to have a stoichiometric ratio $\text{NCO}/\text{OH} = 2$. The reaction is performed in bulk at 80 °C for 4 h under vacuum. The product prepared above was dissolved in tetrahydrofuran (10^{-2} mol for 100 mL) and was immediately combined with the organosilane using a stoichiometric ratio $\text{NCO}/\text{NH}_2 = 1$. The organosilane is added dropwise to prevent a too fast reaction. The mixture was stirred at room temperature for 1 h. The solvent was removed under a rotating evaporator at 40 °C for 15 h. The characteristics of these α,ω silane-terminated macromonomers are reported in Table II. During the first step of the synthesis, there is chain extension resulting in a distribution of molecular weights. But all the chains are terminated exclusively by ethoxysilane groups, with no dead product and with a unique value of functionality of 2 when (γ -aminopropyl)dimethylethoxysilane (γ -APDMES) is used and of 6 with (γ -aminopropyl)triethoxysilane (γ -APS), as shown in Table II.

(ii) The single-end silane-terminated macromonomer was also prepared by a two-step reaction described in a previous paper.²² Diisocyanate IPDI is reacted with monofunctional PEO1 with a stoichiometric ratio $\text{NCO}/\text{OH} = 2$ at 80°C for 24 h, in bulk, without catalyst and under vacuum. Size exclusion chromatography (SEC) of the materials allows us to determine the molar fraction of residual diisocyanate, equal in this case to 0.17 mol. This value, lower than the most probable one, 0.25, has been explained by the different reactivities of the isocyanate groups.²² The product prepared above was dissolved in tetrahydrofuran (10^{-2} mol for 100 mL) and was immediately combined with the organosilane with a stoichiometric ratio $\text{NCO}/\text{NH}_2 = 1$. The mixture was stirred at room temperature for 1 h. An infrared spectrum of the products showed no unreacted isocyanate and thus a complete reaction. The solvent was removed under a rotating evaporator for 15 h at 40°C . Using the previous results,²² the following weight distribution was determined for the reaction product, named PEO1 macromonomer, based on (γ -aminopropyl)triethoxysilane:

γ APS-IPDI- γ APS: 0.17 mol with a functionality of ethoxysilane groups equal to 6

PEO1-IPDI- γ APS: 0.66 mol with a functionality of
ethoxysilane groups equal to 3

PEO1-IPDI-PEO1: 0.17 mol with a functionality equal to 0

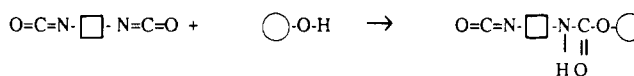
The characteristics of this system are reported in Table II. The number average functionality \bar{f}_n and the functionality average functionality \bar{f}_w were calculated to be 3.6 and 4, respectively.

All the synthesized macromonomers were colorless and transparent. The last system will be useful for studying hydrolysis and condensation reactions. The PEO1-IPDI-PEO1 species, which does not bear reactive groups, is a dead product, but will serve as an internal reference.

We will indifferently use below the terms macromonomer or monomer to designate the products prepared as explained above.

Nomenclature. The nomenclature that was developed can be illustrated by the example shown below: PEO1 ($\bar{f} = 4$) where PEO indicates the type of oligomer used and 1 represents the functionality in hydroxy groups of this oligomer, followed by \bar{f} , the functionality average functionality \bar{f}_w of the macromonomer.

1. synthesis of prepolymer functionalized isocyanate



2. synthesis of alkoxy-silane terminated macromonomer

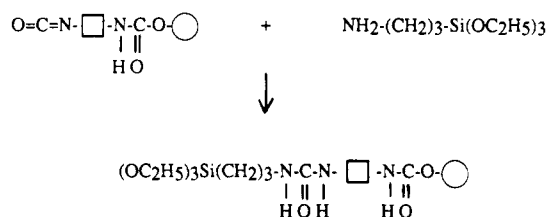


Figure 1. Synthesis of a silane-terminated macromonomer.

Results and Discussion

Reactions of α,ω Silane-Terminated Macromonomers ($\bar{X}_w = 2$). Reactions of α,ω silane-terminated macromonomers have been investigated in order to study the reactivities of alkoxy silane groups. Reactions take place at 40 °C, in bulk, with 3 mol of H₂O to 1 mol of silane, H₂O/Si = 3. Without any catalyst, no reaction occurs, even after several days. Trifluoromethanesulfonic acid (triflic acid, CF₃SO₃H) or hydrochloric acid (HCl) has been used in order to have a catalyst ratio H⁺/Si = 0.05.

Examples of the chromatograms obtained for the system based on γ -APDMES/PEO2 ($\bar{f} = 2$) with triflic acid as the catalyst at different reaction times are shown in Figure 2. The disappearance of the hydrolyzed or partially hydrolyzed macromonomer is very fast and occurs simultaneously with the appearance of an unresolved peak corresponding to products of higher molecular weight. The position of this peak varies with reaction time, but the reaction is too rapid to permit us to follow precisely its molecular weight evolution. For the linear homopolymerization of PEO2 ($\bar{f} = 2$), the number average degree of polymerization \overline{DP}_n is calculated by the ratio $\overline{DP}_n = \bar{M}_n/M_0$ where \bar{M}_n represents the number average molecular weight of the polymer (determined by SEC in our case) and M_0 is the mean molecular weight of the constitution repeating unit ($\bar{M}_n = 793$ g/mol).

After 15 min, the degree of polymerization \overline{DP}_n is higher than 200. As expected in the case of a difunctional monomer, gelation was not observed; even after 1 week, the formed product was still soluble in THF and $CHCl_3$.

In the case of a polycondensation reaction, in the presence of a catalyst and thus a first-order kinetics mechanism, the relation between \overline{DP}_n , the number average degree of polymerization, the extent of reaction (x), and the reaction time (t) is given by¹⁵

$$\overline{DP}_n = \frac{1}{1-x} = C_0 kt + 1 \quad (4)$$

where C_0 is the initial concentration in alkoxy silane groups and k is the condensation rate constant.

In Figure 3, the evolution of the number average degree of polymerization, \overline{DP}_n , is plotted. The curve of \overline{DP}_n as a function of time indicates a polycondensation mechanism, and the slope of this curve gives us a value of k equal to $0.16 \text{ mol}^{-1} \text{ kg s}^{-1}$. This value is only approximative

Table II
Characteristics of Alkoxysilane-Terminated Macromonomers

| macromonomer composition (mol) | notation | \bar{M}_{th} | \bar{M}_n | \bar{M}_w | I_p | f_{OR} |
|------------------------------------|------------------------|----------------|-------------|-------------|-------|--------------------------------------|
| PEO1-IPDI- γ APS (1-1-1) | PEO1 ($\bar{f} = 4$) | 793 | 1309 | 1494 | 1.14 | $\bar{f}_n = 3.6$ $\bar{f}_w = 4$ |
| PEO2-IPDI- γ APDMES (1-2-2) | PEO2 ($\bar{f} = 2$) | 1170 | 990 | 1776 | 1.7 | $\bar{f}_w = 2$ |
| PEO2-IPDI- γ APS (1-2-2) | PEO2 ($\bar{f} = 6$) | 1290 | 1505 | 2604 | 1.7 | $\bar{f}_w = 6$ |

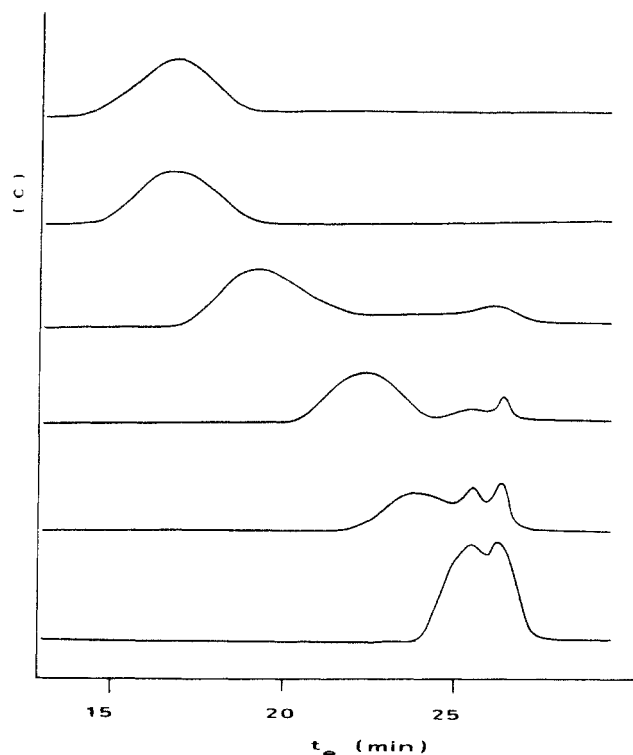


Figure 2. SEC chromatograms at different reaction times for the system PEO2 ($\bar{f} = 2$) at $T = 40^\circ\text{C}$ ($\text{H}_2\text{O}/\text{Si} = 3$ and $\text{H}^+/\text{Si} = 0.05$) with CHCl_3 as the solvent.

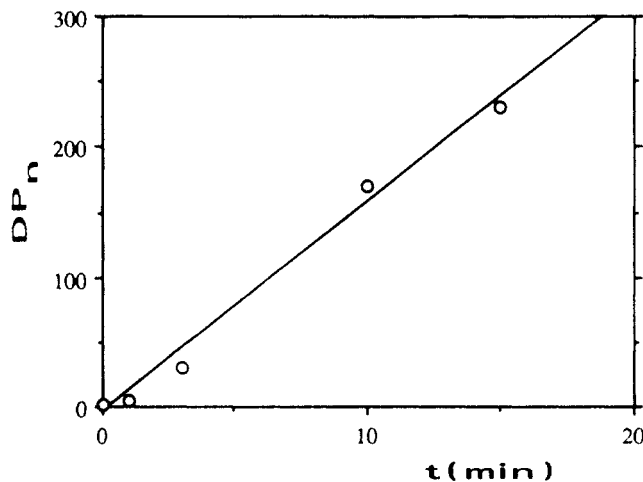


Figure 3. Evolution of $\overline{\text{DP}}_n$ versus time for the system PEO2 ($\bar{f} = 2$) at $T = 40^\circ\text{C}$ ($\text{H}_2\text{O}/\text{Si} = 3$ and $\text{H}^+/\text{Si} = 0.05$).

because of different imprecisions for the $\overline{\text{DP}}_n$ determination (polydisperse macromonomer, polystyrene calibration), but it means that the reaction is very fast at low temperature.

For PEO2 ($\bar{f} = 6$), the disappearance of the hydrolyzed or partially hydrolyzed macromonomer is quasi instantaneous, as shown in Figure 4. Instantaneously, we also noticed the formation of a polymer of high molecular weight ($\bar{M}_n > 400\,000$, $\bar{M}_w/\bar{M}_n = 2.6$ expressed in PS standards) corresponding to a high degree of polymerization. Insoluble fractions in CHCl_3 were produced after

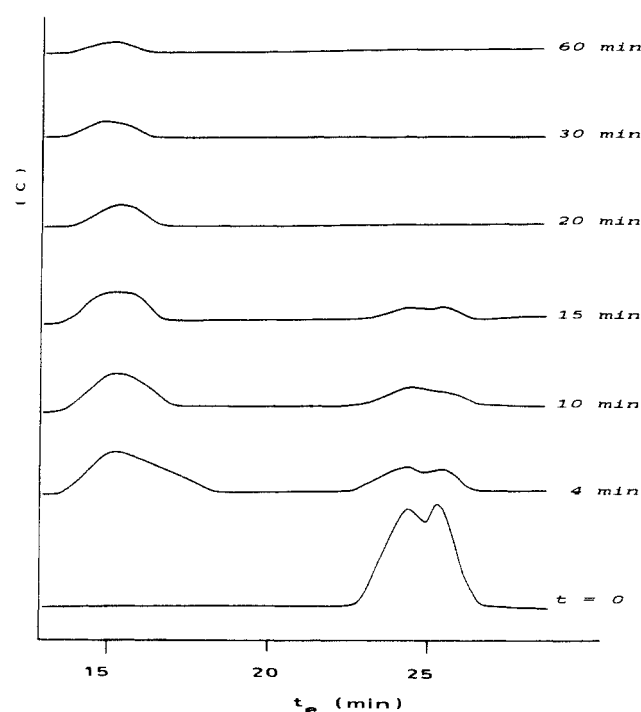


Figure 4. SEC chromatograms at different reaction times for the system PEO2 ($\bar{f} = 6$) at $T = 40^\circ\text{C}$ ($\text{H}_2\text{O}/\text{Si} = 3$ and $\text{H}^+/\text{Si} = 0.05$) with CHCl_3 as the solvent.

10 min of reaction. After 15 min, all the macromonomer has reacted. For α,ω silane-terminated macromonomers, PEO2 ($\bar{f} = 2$) and PEO2 ($\bar{f} = 6$), we obtain a similar behavior: the disappearance of the totally or partially hydrolyzed macromonomer is very fast; in the same time, after a few minutes of reactions, a polymer of high molecular weight appears.

For the PEO2 ($\bar{f} = 2$) system, chain extension is the only reaction possible. Therefore, we can say that the condensation reaction rate for the silanol group of γ -APDMES is in the range $0.10\text{--}0.20\text{ mol}^{-1}\text{ kg s}^{-1}$.

For the PEO2 ($\bar{f} = 6$) system, the second and then the third silanol groups may react with the same or lower condensation rates but lead to a rapid gelation. To increase the gelation time and in order to estimate the different hydrolysis and condensation rates, we are now going to study the reactions of alkoxysilane groups on a compound with a functionality \bar{f}_w higher than 2 but lower than 6.

Reactions of the $\bar{f}_w = 4$ System. Evolution of the Reaction As Determined by ^{29}Si NMR Spectroscopy. Hydrolysis and condensation experiments were also performed at 40°C , in bulk, with 3 mol of H_2O to 1 mol of silane and a catalyst ratio $\text{H}^+/\text{Si} = 0.05$. At different reaction times, about 3 g of the samples was extracted and dissolved in CDCl_3 (3 g) and the ^{29}Si NMR spectrum examined immediately after. For each sample, the reaction time was defined as the time interval between the initial addition of the acid and water to the reactive system and the addition of the solvent CDCl_3 . The ^{29}Si NMR spectrum of the alkoxysilane-terminated macromonomer PEO1 ($\bar{f} = 4$) is shown in Figure 5. The resonance at -45 ppm corresponds to a silicon atom directly coordinated to three

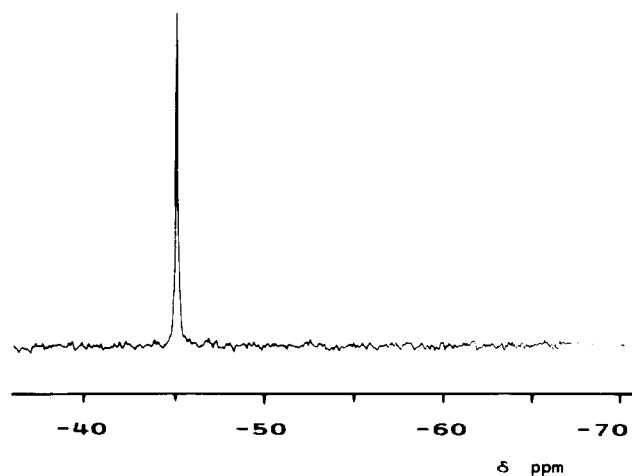


Figure 5. ^{29}Si NMR spectrum of alkoxy silane-terminated macromonomer PEO1 ($f = 4$) in deuteriochloroform CDCl_3 .

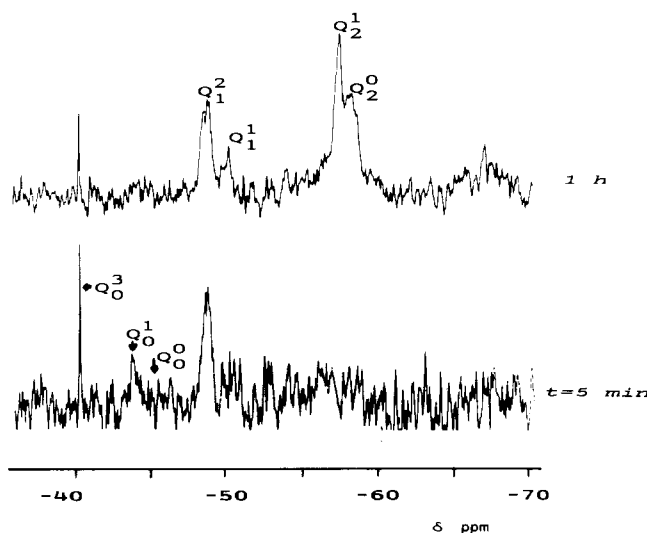
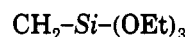


Figure 6. ^{29}Si NMR spectra at different reaction times for the system PEO1 ($f = 4$) at $T = 40^\circ\text{C}$ ($\text{H}_2\text{O}/\text{Si} = 3$ and $\text{H}^+/\text{Si} = 0.05$) with HCl as the catalyst.

ethoxysilane groups and one methylene carbon:



The NMR spectra evolve quickly when a catalyst is used. Figure 6 shows representative spectra for the case when HCl is used as the catalyst. At the initial hydrolysis stage, corresponding to a reaction time as previously defined, $t = 5$ min, the relative intensity of the peak of starting material ($\delta = -45$ ppm with respect to TMS) decreased rapidly. The intensity of the hydrolyzed monomer species ($\delta = -40$ ppm and probably $\delta = -44$ ppm) increased at the same rate. The spectra were not quantified because the signal to noise ratio is too low in this case.

The chemical shifts are functions of the state of alkoxy silane polymerization. Peak assignments of the silicon atom depend on the next-to-nearest neighbor of the silicon atom being observed. With this approach, the degree of hydrolysis and condensation of a given silicon species can be determined. Since the hydroxide is more electron withdrawing than the ethoxide, the peaks to higher field are attributed to the hydrolyzed species; the more Si-(OEt)_3 is hydrolyzed, the higher field it resonates. It was possible to observe all the intermediate hydrolyzed species corresponding to different degrees of hydrolysis such as



Condensation of the hydrolysis products (eqs 2 and 3) results in an upfield, lower ppm shift of ^{29}Si NMR

Table III
Indexation of ^{29}Si NMR Peaks

| species | formulas | nomenclature | δ (ppm) ²² |
|---|--|----------------|------------------------------|
| nonhydrolyzed monomer | $\text{CH}_2\text{Si(OEt)}_3$ | Q_0^0 | -45 |
| hydrolyzed monomeric species | $\text{CH}_2\text{Si(OH)}_3$ | Q_0^3 | -40 |
| hydrolyzed and partially hydrolyzed dimers | $\text{CH}_2\text{Si(OEt)}_2\text{(OH)}$ | Q_0^1 | -44 |
| | OH | Q_1^2 | -48 |
| | $\text{CH}_2\text{Si/OSi}$ | | |
| | OH | | |
| hydrolyzed and partially hydrolyzed trimers | OH | Q_1^1 | -50 |
| | $\text{CH}_2\text{Si/OSi}$ | | |
| | OEt | | |
| | OH | Q_2^1 | -56.5 |
| hydrolyzed and partially hydrolyzed tetramers | $\text{CH}_2\text{Si/OSi}$ | | |
| | O | | |
| | Si | | |
| | OEt | Q_2^0 | -58 |
| hydrolyzed and partially hydrolyzed tetramers | $\text{CH}_2\text{Si/OSi}$ | | |
| | O | | |
| | Si | | |
| | O | Q_3^0 | -64 |

resonances. It was possible to identify the chemical shifts by comparing them to the numerous identifications found in the literature,^{1,23-27} mainly those given by Nishiyama et al.²³ These authors have studied the hydrolysis and the condensation of (γ -(methacryloxy)propyl)triethoxysilane (γ MPTS) by ^{13}C and ^{29}Si NMR spectroscopy. The chemical shifts corresponding to different degrees of condensation (dimer, one siloxane bond; trimer, two siloxane bonds; tetramer, three siloxane bonds) have been identified. For each condensation species, different degrees of hydrolysis are visible, as we will see later. The nomenclature used here is Q_Z^Y , where Z represents the number of siloxane bonds and Y the number of hydroxyl groups on a given silicon atom.

In agreement with previous results,^{28,29} for a typical acid-catalyzed sol-gel system, the disappearance of the monomer by hydrolysis is essentially complete in less than 3 min and the condensation already started. This time is comparable to the time required to prepare the sample and record a spectrum. In that case, the hydrolysis reaction was too rapid to allow us to observe the evolution of all the intermediate hydrolyzed species corresponding to different degrees of hydrolysis. One type of hydrolyzed monomer species Q_0^3 is observed at -40 ppm and most likely corresponds to a probably completely hydrolyzed species, as shown in Table III. Another resonance which is very weak is detected at -44 ppm and corresponds to the Q_0^1 species.

If the hydrolysis stage is very short, condensation takes more time. When triflic acid was used as the catalyst, we were not able to observe the hydrolysis reaction. The other peaks observed in Figure 7, and corresponding to different degrees of condensation, will be discussed now.

After a reaction time of 10 min (Figure 7), no more residual monomer (-45 ppm) and no more hydrolyzed monomeric product (-40 ppm) are visible. On the basis of the previous results,²³ Table III shows assignments for a silicon

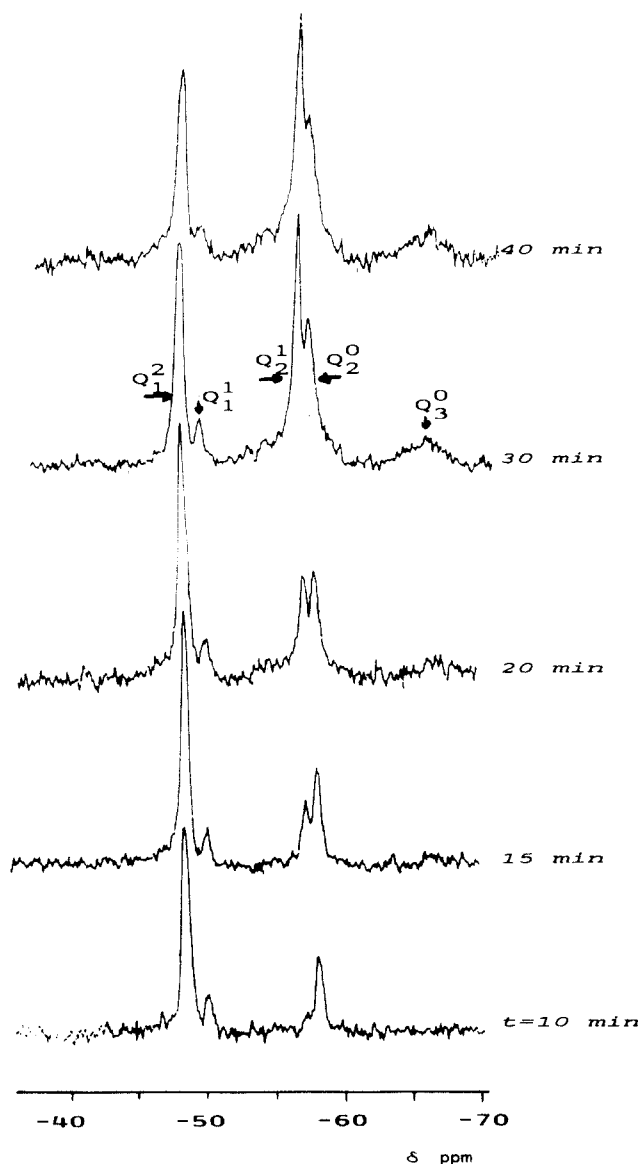


Figure 7. ^{29}Si NMR spectra at different reaction times for the system PEO1 ($f = 4$) at $T = 40^\circ\text{C}$ ($\text{H}_2\text{O}/\text{Si} = 3$ and $\text{H}^+/\text{Si} = 0.05$) with $\text{CF}_3\text{SO}_3\text{H}$ as the catalyst.

atom in different environments. (i) Peaks at -48 ppm are attributed to a silicon atom with one siloxane bond corresponding to the dimer species with different degrees of hydrolysis, as defined in Table III and assigned to Q_1^2 (hydrolyzed dimer) and Q_1^1 (partially hydrolyzed dimer) peaks by referring to previous results.²³ (ii) At -58 ppm, the peaks observed are assigned this time to a silicon atom with two siloxane bonds corresponding to the trimer species Q_2^1 and Q_2^0 with different degrees of hydrolysis. (iii) A broad resonance is observed at -68 ppm: this resonance is assigned to a silicon atom with three siloxane bonds and corresponding to the tetramer species Q_3^0 . The width of this resonance can be explained by a lower mobility of these species compared to the others.

Depending on polymerization time, the relative areas of the different peaks on the ^{29}Si NMR spectrum for hydrolyzed or nonhydrolyzed i -mers are shown in Figure 8 and are representative of the main mechanisms of hydrolysis and condensation. The monomer hydrolysis is instantaneous, as we have seen earlier. We are not able to evaluate the degree of hydrolysis on each chain end, but the percentage of residual alkoxy silane groups can be estimated by the relative intensities of the Q_2^0 and Q_1^1 species. After 10 min, the areas of the Q_2^0 and Q_1^1 species, respectively, are equal to 25% and 8% of the total area.

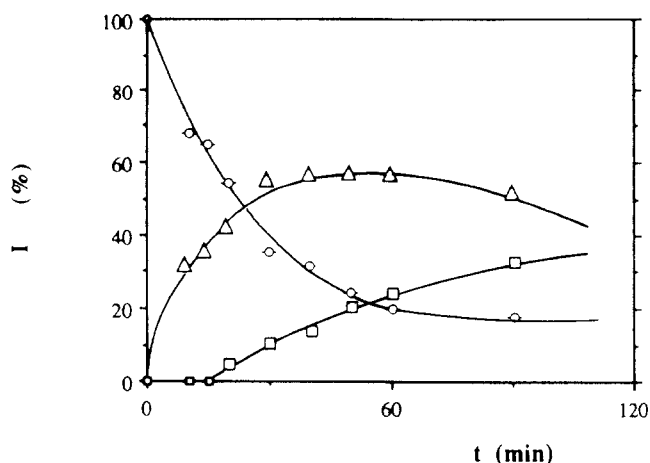


Figure 8. Relative intensities of the ^{29}Si atom of γ -APS at $T = 40^\circ\text{C}$ ($\text{H}_2\text{O}/\text{Si} = 3$ and $\text{H}^+/\text{Si} = 0.05$): (O) dimer Q_1 ; (Δ) trimer Q_2 ; (\square) tetramer Q_3 .

So, the percentage of nonhydrolyzed alkoxy silane groups is equal to 33:3–11%. The appearance of the condensate dimer species was as fast as the disappearance rate of the hydrolyzed product. The dimer species then decreased rapidly with an increase in trimer species, and finally, the peak attributable to the tetramer increased with a decrease in the trimer peaks. These results, presented in Figure 8, are partially complete because we have no indication about the disappearance of the starting material and hydrolyzed monomeric products, except that they occur rapidly.

Evolution of the Reaction As Determined by SEC. As the functionality of our monomer is higher than 2, gelation can occur. The gel point is defined as the conversion at which the weight average molecular weight \bar{M}_w diverges and an infinite network begins to be formed which is insoluble in any solvent. Therefore, SEC is a suitable method to determine the gel time and the monomer conversion at the gel point during the same experiment. After a given time at an isothermal curing temperature ($T_i = 40^\circ\text{C}$), 0.1-g samples are dissolved in 10 mL of THF or CHCl_3 . The solution is filtered through a Millipore membrane ($0.2\ \mu\text{m}$) and gelation is taken as the point when the filter becomes plugged. The solution is analyzed by SEC to obtain the variations of molar mass as a function of time. Examples of the chromatograms obtained for the studied system at different reaction times are shown in Figure 9 for both solvents.

In THF as the solvent, we observed only one peak at $t_e = 21.9$ min at different reaction times. This peak has the same elution time as the initial silane-terminated monomer. Keep in mind that after 10 min of reaction, no residual monomer was visible in the ^{29}Si NMR spectra (Figure 7); we were obliged to attribute this peak to the dimer and to conclude that the elution times for the nonhydrolyzed or hydrolyzed monomer and the dimer are the same. As time increased, the intensity of this peak decreased, while no more products of higher molecular weight were visible. However, in this case, insoluble fractions were produced after 20 min at 40°C . On the contrary, in chloroform as the solvent, several peaks are observed. The peak at $t_e = 25.1$ min is attributed to the dimer for the same reasons as discussed previously (no more residual monomer visible in the NMR spectra). The unresolved peak at lower elution times ($t = 22$ min) can be attributed to trimers and oligomers. The height of this peak decreases with time, but its position does not change and corresponds to a degree of polymerization equal to about 3–4. After 10 min of reaction, a new peak at $t_e = 15$ min was noticed, corresponding to a product of high

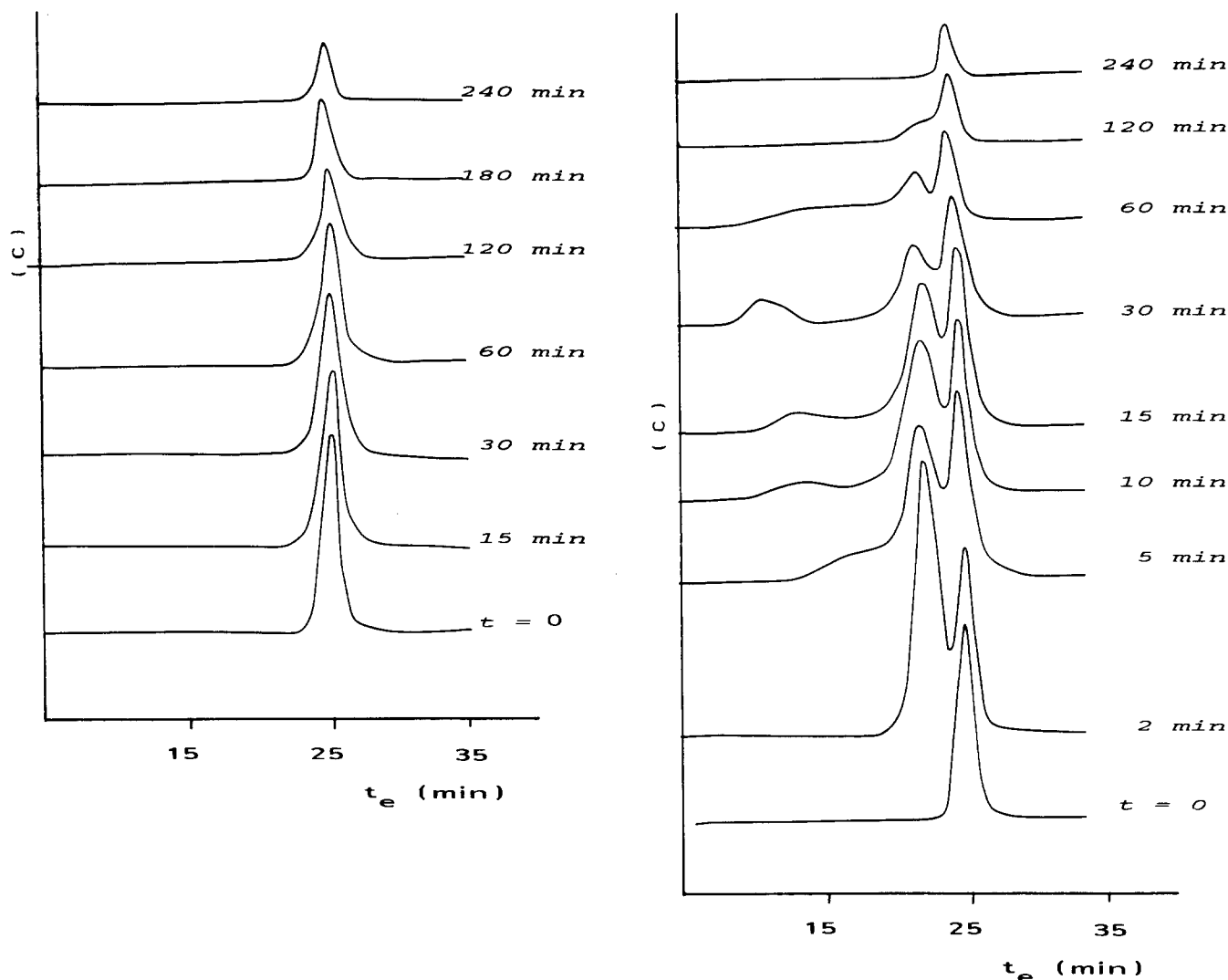


Figure 9. SEC chromatograms at different reaction times for the system PEO1 ($\bar{f} = 4$) at $T = 40^\circ\text{C}$ ($\text{H}_2\text{O}/\text{Si} = 3$ and $\text{H}^+/\text{Si} = 0.05$) with (a, left) THF and (b, right) CHCl_3 as the solvents.

molecular weight ($\bar{M}_n > 50\,000$ expressed in PS standards). As in the preceding case, insoluble fractions were observed after 20 min.

The combination of the SEC and NMR results permits us to discuss the mechanisms of the polymerization. The information on the molecular weight evolution obtained by SEC with THF as the solvent is not complete. We can state that products of higher molecular weight are not apparent because they have the same refractive index as the solvent (THF). In the case of CHCl_3 , the molecular weight evolution looks like that obtained for α,ω silane-terminated macromonomers: (i) immediate disappearance of monomer and instantaneously appearance of the dimer species; (ii) appearance of trimers and tetramers at slower rates; (iii) appearance of high-molecular-weight species just before and after the gelation phenomenon. After the gel point, we have only the chromatogram of the soluble fraction.

Finally, the molecular weight evolution looks like a classical polycondensation reaction, with some proper characteristics. During the initial stages of polymerization, we have chain extension, corresponding to the appearance of the dimer and trimer species as we can see in Figure 10. As the reaction time increases, the appearance of the product of high molecular weight ($\bar{M}_n > 50\,000$) corresponds to the appearance of the tetramer species, observed at $t = 20$ min just before the gelation. The disappearance of the dimer can be characterized using the

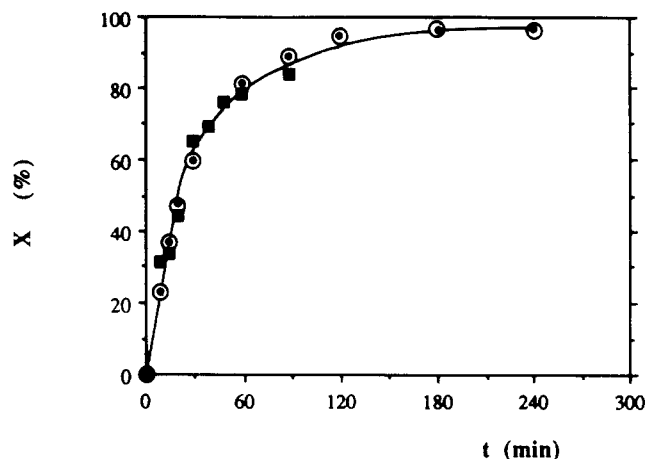


Figure 10. Dimer conversion vs reaction time at $T = 40^\circ\text{C}$ ($\text{H}_2\text{O}/\text{Si} = 3$ and $\text{H}^+/\text{Si} = 0.05$): (●) solvent THF; (○) solvent CHCl_3 ; (■) ^{29}Si NMR data.

NMR and SEC results. In the case of SEC we must take into account the height of the peak y of the dead product PEO1-IPDI-PEO1. This species, which does not bear reactive groups, has the same elution time as the dimer and its concentration stays constant during the entire reaction. So, the disappearance of the dimer is given by the following equation:

$$X = 1 - (h_t - y)/(h_0 - y) \quad (5)$$

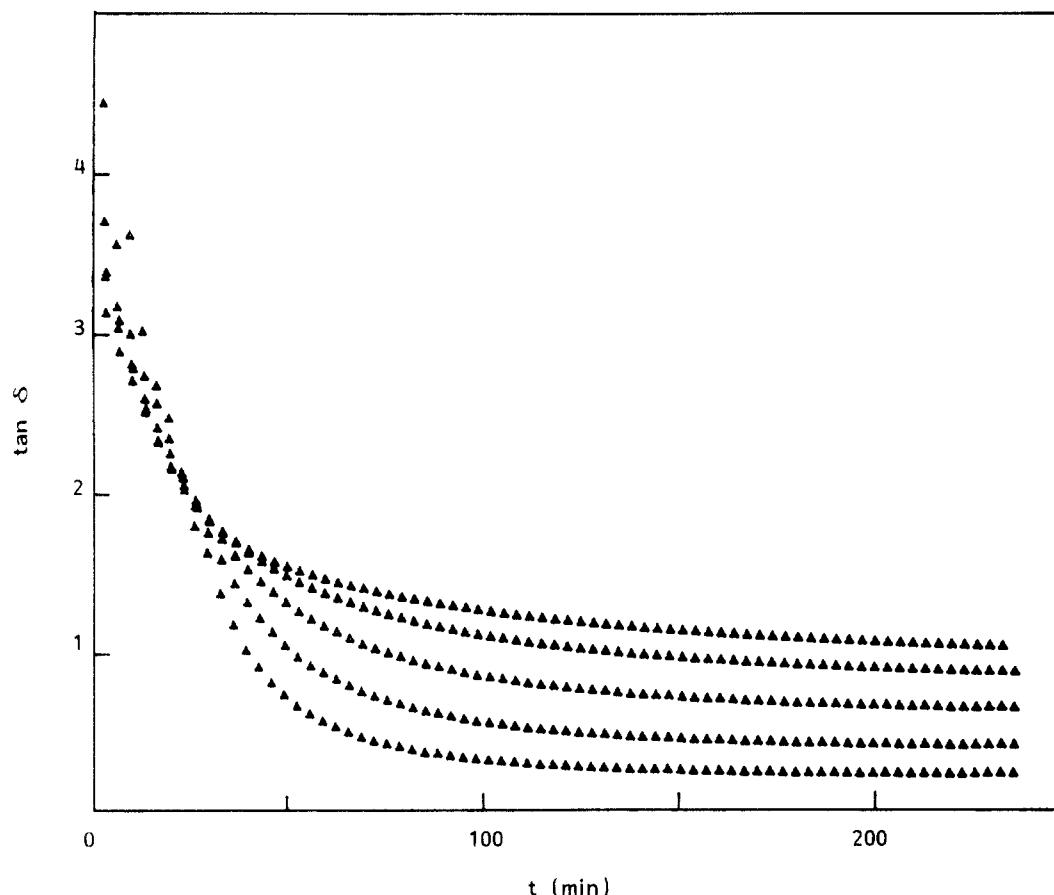


Figure 11. Loss factor $\tan \delta$ at five angular frequencies (2.5, 7.9, 25, 79, 250 rad/s) for the monomer PEO1 ($\bar{f} = 4$) at $T = 40^\circ\text{C}$ ($\text{H}_2\text{O}/\text{Si} = 3$ and $\text{H}^*/\text{Si} = 0.05$).

with h_t being the height of the dimer peak at t . And for NMR spectroscopy

$$X = 1 - (I_t/I_0) \quad (6)$$

with I being the area of the peak at -48 ppm.

The conversion of the dimer as calculated by both methods is plotted as a function of time in Figure 10. We observed a good agreement between the SEC and NMR experiments. This result fits our hypothesis and confirms our choice of the assignments of the SEC peaks.

Gelation. Insoluble fractions in THF and CHCl_3 were obtained after 20 min. We also determined the gel point by dynamic mechanical measurements. The evolution of our system was followed starting immediately after mixing and proceeding through the macroscopic gel point, corresponding to the appearance of insoluble fractions.

It has been suggested that for some polymers,³¹ G' is equal to G'' at the gel point, regardless of the frequency. Our data show the crossover of G' and G'' after the macroscopic gel point. The G' and G'' crossover shows some frequency dependence ($t_{G'=G''}$ increases with an increase in frequency), although the dependence may be ambiguous. The process of gelation is demonstrated in Figure 11, where the loss tangent $\tan \delta = G''/G'$ is shown as a function of time for five frequencies ranging from 2.5 to 250 Hz. One single crossing point of the five curves exists at $\tan \delta \sim 2 \pm 0.2$. Such observations were made by several authors.¹⁷⁻²¹ These authors claim from theoretical arguments that this crossover point is the gel point, but the values for $\tan \delta$ depend on the system. This crossover point, considered to be the gel point, is located at $t = 23 \pm 3$ min in our case and coincides with the time determined by the appearance of insolubles in THF and CHCl_3 . The viscoelastic component may be calculated

with the following equation:

$$G''/G' = \tan \delta = \tan (\Delta\pi/2) \quad (7)$$

with $\tan \delta$ being the value at the crossing point and Δ the scaling exponent. The values found for Δ are between 0.68 and 0.65 for $t = 23 \pm 3$ min. In order to calculate Δ more precisely, the variations in $\log G'$ and $\log G''$ against $\log \omega$ are represented in Figure 12a,b for several measurement times near the gelation critical point. The slopes of these lines yield the value of Δ , the viscoelastic exponent at the gel point, as follows:

$$G' \propto G'' \propto \omega^\Delta \quad (8)$$

for the frequency dependence of the moduli.

As noted in the Introduction, values of Δ near the critical gelation point are predicted by various theories. In our case, we found $\Delta = 0.63 \pm 0.02$. This value is in good agreement with the percolation theory and previously measured values for epoxy resins,^{17,18,30,32} polyurethanes (PU),^{19,20} and polyesters.³³ The results are not consistent with predictions by the Flory-Stockmayer mean-field theory ($\Delta = 1$)¹⁸ nor with experimental work for the cross-linking of PDMS with an excess of the cross-linking agent ($\Delta = 0.5$).^{31,34} As we have said in the Introduction, for PU at stoichiometric conditions, Muller et al.²⁰ found $\Delta = 0.5$, but when a given amount of zero functional polyether α,ω -dimethyl ether (not involved in the urethane reaction) is introduced, they have $\Delta = 0.67$. To explain these results, they consider that the response of the "infinite" macromolecule, specifically its distribution of relaxation times, will depend upon its environment. In our case, we also have zero functional dead oligomers, PEO1-IPDI-PEO1 (17% by mole).

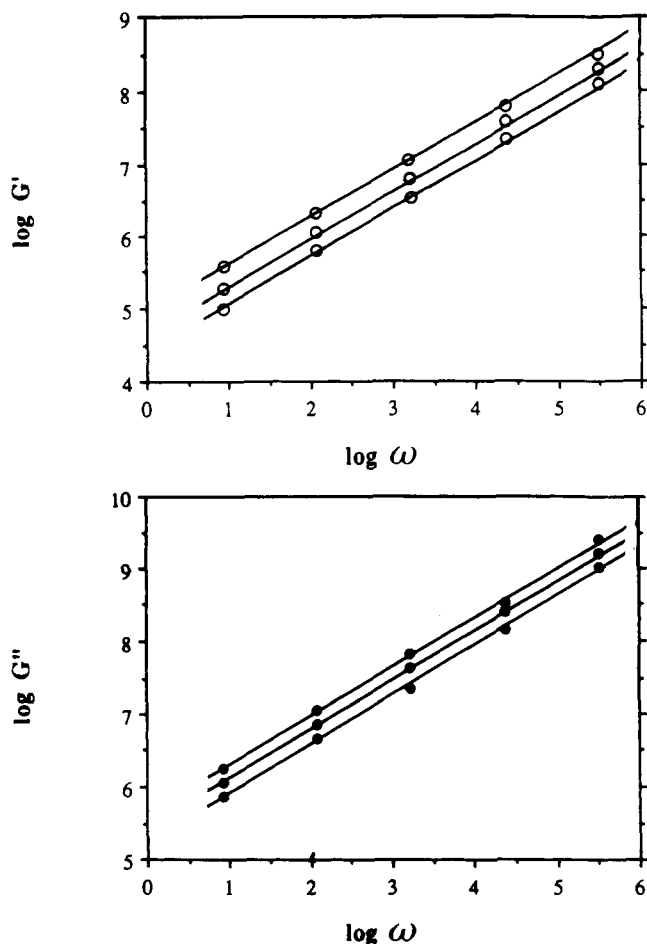


Figure 12. log plot of (a, top) G' and (b, bottom) G'' against measurement frequencies at times of 20, 23, and 26 min from the bottom to the top.

However, this viscoelastic method is suitable for determining gel times and we can consider that the gelation time occurs after 20–23 min of reaction in our system.

We can now calculate the conversion degree of reactive groups at the gel point, using the relative areas of the dimer, trimer, and tetramer peaks determined by ^{29}Si NMR spectroscopy.

Assuming that (i) we have no more reactive monomer and (ii) the areas of the peaks at -48 (Q_1), -58 (Q_2), and -68 ppm (Q_3) (see Figure 7) are proportional to the number of silicon atoms with one, two, and three siloxane bonds, we can calculate the conversion degree, x , with the following equation:

$$x(t) = \frac{[\text{dimer}] + 2[\text{trimer}] + 3[\text{tetramer}]}{3} \quad (9)$$

where $[i\text{-mer}]$ is the concentration of the i -mer species at t .

In Figure 13, x is plotted as a function of time. At the first reaction stages, the conversion increases at a very fast rate from 0 to 0.35 due to the fast formation of the dimer. At 40°C the gel time, t_{gel} , is equal to 20–23 min and the conversion is about 50%. If we consider the homopolymerization of the prepolymer bearing \bar{f}_w reactive groups, we can calculate x_{gel} , the conversion at the point gel:³⁵

$$x_{\text{gel}} = \frac{1}{\bar{f}_w - 1} \quad (10)$$

In our case, the weight average functionality, \bar{f}_w , of the initial reactive oligomer is equal to 4, so the theoretical conversion at gelation is equal to 0.33.

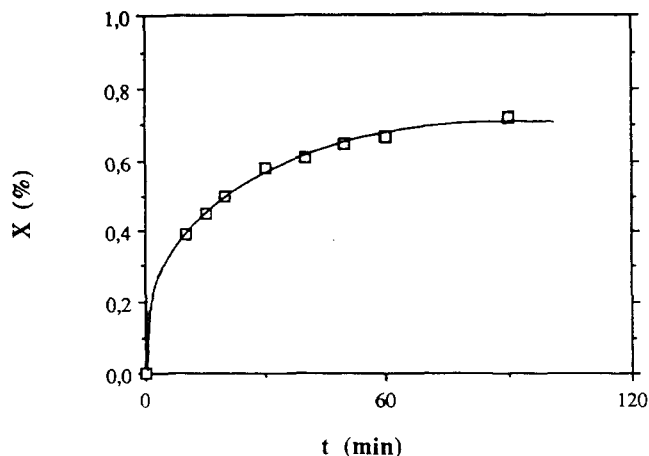
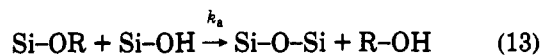
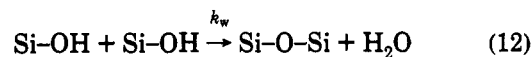
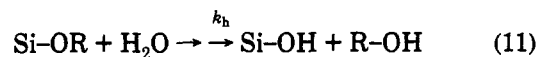


Figure 13. Reactive group conversion versus reaction time.

The difference between the theoretical and experimental conversion at the gel point can be explained by a substitution factor, r , of less than 1 and by cyclization reactions. This point will be discussed later.

Discussion

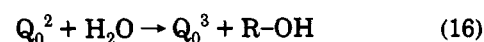
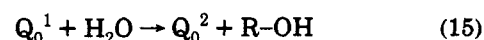
The kinetics of sol-gel reactions can be formulated at different levels. The simplest kinetics model considers only the concentrations of the various functional groups (alkoxy, silanol, and siloxane Si-O-Si), without reference to how they are distributed about the various silicon atoms. So, only three types of reactions are necessary to formulate the functional group rate equations:



These reactions are referred as the hydrolysis (h), water-producing condensation (w), and alcohol-producing condensation (a).

Hydrolysis Reaction (Case of $\bar{f}_w = 4$ Macromonomer PEO1). When $\text{CF}_3\text{SO}_3\text{H}$ is used as the catalyst, the hydrolysis reactions were too fast to allow us to observe all of the intermediate hydrolyzed species, corresponding to Q_0^1 , Q_0^2 and Q_0^3 species.

When HCl is used as the catalyst, the signal to noise ratio is too poor to estimate the area of the peaks. The starting reactant completely disappeared before measurements could be made. The following hydrolysis reactions are possible:



We will assume that the hydrolysis reactions are not balanced. On the basis of a second-order hydrolysis kinetics, only a lower limit for the hydrolysis rate constant k_h of the Q_0^0 species can be calculated. The corresponding rate expression for the reactions of the functional

groups can be written as

$$-\frac{d[Q_0^0]}{dt} = 3k_h[Q_0^0][H_2O] \quad (17)$$

where k_h is the hydrolysis rate constant, $[Q_0^0]$ is the concentration of the Q_0^0 monomer species (mol/kg), and $[H_2O]$ is the water concentration (mol/kg). At the beginning of the reaction, the water concentration is $[H_2O]_0 = 3[Q_0^0]_0$.

In the limiting case where the overall condensation is negligible with respect to the hydrolysis rate, we can write

$$-\frac{d[Q_0^0]}{dt} = 9k_h[Q_0^0]^2 \quad (18)$$

After 5 min of reaction, no more Q_0^0 specie is apparent (ratio NMR signal to noise is too weak), so we can estimate the value of $[Q_0^0]_t$ in the range $0.01[Q_0^0]_0$ – $0.05[Q_0^0]_0$. The resolution of this equation (17) gives us limiting values of k_h :

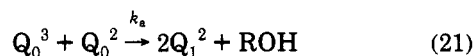
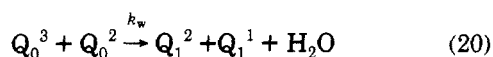
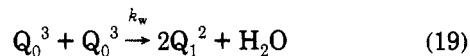
$$k_h > 3 \times 10^{-2} \text{ mol}^{-1} \text{ kg s}^{-1} \text{ for } [Q_0^0]_t = 0.01[Q_0^0]_0$$

$$k_h > 6 \times 10^{-3} \text{ mol}^{-1} \text{ kg s}^{-1} \text{ for } [Q_0^0]_t = 0.05[Q_0^0]_0$$

This k_h value is greater or in the same order than that obtained by Assink et al.²⁸ ($k_h = 6.10 \times 10^{-3} \text{ mol}^{-1} \text{ L s}^{-1}$) for TEOS-HCl-catalyzed reactions.

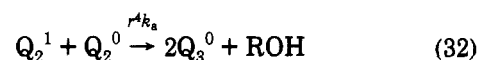
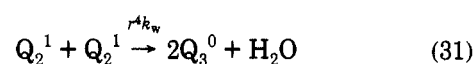
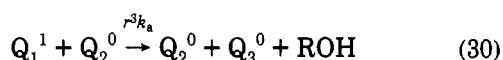
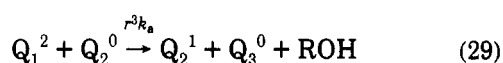
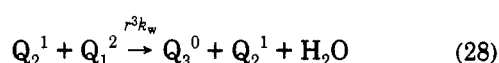
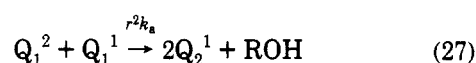
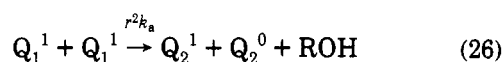
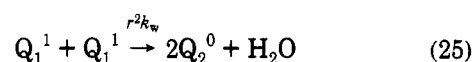
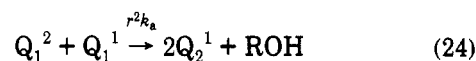
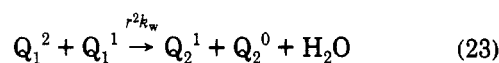
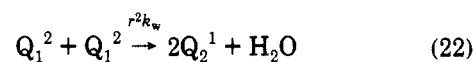
Condensation Reaction. From the results of the condensation of the PEO2 ($\bar{f} = 2$) macromonomer, the condensation reaction rate k has been estimated equal to $0.16 \text{ mol}^{-1} \text{ kg s}^{-1}$. This k value, determined by assuming a second-order kinetics law (eq 4) represents the condensation rate for the silanol group of monofunctional silane coupling agent γ -APDMES. The NMR results for the PEO1 ($\bar{f} = 4$) macromonomer indicate that the peak intensities for the dimer and trimer species reach a maximum concentration during the initial hours of reaction, as shown in Figure 8. The time taken to reach the maximum concentration increases with the degree of polymerization: the reactivity of residual silanol groups depends on the degree of polymerization, in agreement with preceding results.

With triflic acid as the catalyst, after 10 min of reaction, the species Q_1^2 , Q_1^1 , Q_2^1 , Q_2^0 , and Q_3^0 are present, where Q_1^1 is always weak and Q_2^0 does not change very much with time. At this time, there are no more reactions involving Q_0^0 and no more hydrolyzed monomeric species are apparent. So, we can conclude that the hydrolysis reactions are terminated but also that condensation reactions such as follows were accomplished:



The reaction rate for the condensation of unreacted monomers is as stated above. However, the condensation rate for species with one siloxane bond is reduced by a value equal to the substitution factor r . The condensation rate for species with two siloxane bonds is reduced by a factor r^2 . This corrective parameter modifies the reactivity of condensed species in proportion to the degree of condensation, in agreement with previous suggestions.⁷

Therefore, we can write the set of equations



The Q_2^0 species concentration does not change very much with time, so we can deduce that k_a is small compared to k_w , in agreement with eq 27, and we will neglect the alcohol-producing condensation. The Q_1^1 species concentration is low in comparison to the Q_1^2 species concentration, so reactions involving Q_1^1 will not be taken into account for the kinetics calculation. With these hypotheses, the reactions that we will be considered are those given by eqs 22, 28, and 31.

The corresponding rate expressions for the functional group reactions can be written as

$$-\frac{d[X]}{dt} = 8r^2 k_w [X]^2 + 2r^3 k_w [XY] \quad (33)$$

$$\frac{d[Y]}{dt} = 8r^2 k_w [X]^2 - 2r^4 k_w [Y]^2 \quad (34)$$

$$\frac{d[Z]}{dt} = 2r^3 k_w [XY] + 2r^4 k_w [Y]^2 \quad (35)$$

$$X = Q_1^2 \quad Y = Q_2^1 \quad Z = Q_3^0$$

We determined the values of r and k_w that best fit the experimental data by numeric calculation. r was determined to be 0.26 and k_w is found equal to $0.06 \text{ mol}^{-1} \text{ kg s}^{-1}$. The value of k_w is relatively large, compared with the values found in the literature ($k_w = 10^{-4} \text{ mol}^{-1} \text{ L s}^{-1}$) for acid-catalyzed systems.²⁸ However, the experimental conditions are different, notably the nature and the concentration of the acid catalyst. Our value of k_w is on the same order as the value determined for the difunctional macromonomer PEO2 ($\bar{f} = 2$) using experimental

equal to 0.5. So, gelation was never reached and these results²⁷ confirm that it is not the gelation process which decelerates the cross-linking process but the vitrification.

As discussed before, the recursive solution of random branching allows substitution effects on the kinetics and permits the calculation of the substitution factor r . Although the kinetic-recursive model is not exact in predicting the molecular weight evolution versus conversion and does not take into account the structural transformations occurring during polymerization, its results provide a basis for understanding future works.

Conclusions

The mechanisms of hydrolysis and condensation reactions of alkoxysilane-terminated macromonomers were investigated by both ²⁹Si NMR and SEC measurements. The condensation reactions are catalyzed by H⁺, as hydrolysis reactions.

The reactivity of functional groups in an $\bar{f}_w = 4$ system depends on how many of the functional groups have been condensed. By examining the molecular weight evolution and the appearance of the different condensed species, we observed a decrease in the condensation rate constants of silanol groups with an increase in the degree of condensation.

The value of the lower limit of the hydrolysis rate is calculated, as the values of the condensation rate and substitution factor, using a simple kinetics model.

The gel time was determined by the appearance of insoluble fractions and by dynamic mechanical experiments. The scaling exponent Δ is found to be 0.63, which is in agreement with the percolation theory. The extent of reaction may be calculated from these results. The conversion at gelation is 0.50; the theoretical conversion at gelation is found to be 0.33. Substitution effects (non-equal reactivity of all the silanol groups) and intramolecular reactions may explain these differences. Substitution effects are increased by phase separation and vitrification. The substitution factor, r , is an adjustable parameter taking into account not only the kinetics substitution effects but also the effects due to structural transformations.

The characterization of these organic-inorganic hybrid materials is in progress in our laboratory. The results about the morphology will soon be published.

Acknowledgment. This work was sponsored by the Corning Europe Co. The financial support of this institution is gratefully acknowledged. We wish to thank H. Watton and R. Petiaud from CNRS (Solaize) for performing and discussing NMR experiments. Special thanks are given to R. J. J. Williams from INTEMA (Mar del Plata) for discussions.

References and Notes

- (1) Hoh, K. P.; Ishida, H.; Koenig, J. L. *Polymer Compos.* **1990**, *11*, 121-125.
- (2) Serier, A.; Pascault, J. P.; Lam, T. M. *J. Polym. Sci. Chem.* **1991**, *29*, 1125-1131.
- (3) Schmidt, H.; Seiferling, B. *Mater. Res. Soc. Symp. Proc.* **1986**, *73*, 739-750.
- (4) Ravaine, D.; Seminel, A.; Charbouillot, Y.; Vincens, M. *J. Non-Cryst. Solids* **1986**, *82*, 210-219.
- (5) Huang, H. H.; Wilkes, G. L.; Carlson, J. G. *Polymer* **1989**, *30*, 2001-2012.
- (6) Livage, J.; Henry, M.; Sanchez, C. *Prog. Solid State Chem.* **1988**, *18*, 259-341.
- (7) Bailey, J. K.; Macosko, C. W.; McCartney, M. L. *J. Non-Cryst. Solids* **1990**, *125*, 208-223.
- (8) Keefer, K. D. *Adv. Chem. Ser.* **1990**, *224*, 227-240.
- (9) Brinker, C. J.; Scherer, G. W. *J. Non-Cryst. Solids* **1985**, *70*, 301-322.
- (10) Keefer, K. D. *Mater. Res. Soc. Proc.* **1984**, *32*, 15-24.
- (11) Strawbridge, I.; Craievich, A. F.; James, P. F. *J. Non-Cryst. Solids* **1985**, *72*, 139-157.
- (12) Yoldas, B. E. *J. Non-Cryst. Solids* **1986**, *83*, 375-390.
- (13) Artaki, I.; Zerda, T. W.; Jonas, J. *J. Non-Cryst. Solids* **1986**, *81*, 381-395.
- (14) Colby, M. W.; Osaka, A.; MacKenzie, J. D. *J. Non-Cryst. Solids* **1988**, *99*, 129-139.
- (15) Flory, P. J. *Principles of Polymer Chemistry*; Cornell University Press: Ithaca, NY, 1953.
- (16) Stauffer, D.; Coniglio, A.; Adams, M. *Adv. Polym. Sci.* **1982**, *44*, 103.
- (17) Adoff, D.; Martin, J. E.; Wilcoxon, J. P. *Macromolecules* **1990**, *23*, 527-531.
- (18) Adoff, D.; Martin, J. E. *Macromolecules* **1990**, *23*, 3700-3704.
- (19) Durand, D.; Delsanti, M.; Adam, M.; Luck, J. M. *Europhys. Lett.* **1987**, *3*, 297.
- (20) Muller, R.; Gerard, E.; Dugand, P.; Rempp, P.; Gnanou, Y. *Macromolecules* **1991**, *24*, 1321-1326.
- (21) Hodgson, D. F.; Amis, E. J. *Macromolecules* **1990**, *23*, 2512-2519.
- (22) Surivet, F.; Lam, T. M.; Pascault, J. P. *J. Polym. Sci., Polym. Chem.*, to be published.
- (23) Nishiyama, N.; Horie, K.; Asakura, T. *J. Appl. Polym. Sci.* **1987**, *34*, 1619-1630.
- (24) Carajaval, G. S.; Leyden, D. E.; Maciel, G. E. In *Silanes, Surfaces and Interfaces*; Leyden, D. E., Ed.; Gordon and Breach Science: New York, 1985; p 283.
- (25) De Haan, J. W.; Van der Bogaert, H. M.; Ponjeé, J. J.; Van de Ven, L. J. M. *J. Colloid Interface Sci.* **1986**, *110*, 591-600.
- (26) Doughty, D. H.; Assink, R. A.; Kay, B. D. *Adv. Chem. Ser.* **1990**, *224*, 241-250.
- (27) Long, T. E.; Kelts, L. W.; Turner, S. T.; Wesson, J. A.; Mourey, T. H. *Macromolecules* **1991**, *24*, 1431-1434.
- (28) Assink, R. A.; Kay, B. D. *J. Non-Cryst. Solids* **1988**, *99*, 359-370.
- (29) Kay, B. D.; Assink, R. A. *J. Non-Cryst. Solids* **1988**, *104*, 112-122.
- (30) Feve, M. *Makromol. Chem., Makromol. Symp.* **1989**, *30*, 95-107.
- (31) Winter, H. H. *Polym. Eng. Sci.* **1987**, *27*, 1698-1702.
- (32) Matejka, L. *Polym. Bull.* **1991**, *26*, 109-116.
- (33) Rubinstein, M.; Colby, R. H.; Gillmor, J. R. *Polym. Prepr.* **1989**, *30*, 81-82.
- (34) Chambon, F.; Winter, H. H. *Polym. Bull.* **1985**, *13*, 499-503.
- (35) Miller, D. R.; Macosko, C. W. *Macromolecules* **1976**, *9*, 206-211.
- (36) Huang, H. H.; Wilkes, G. L. *Polym. Bull.* **1987**, *18*, 455-462.
- (37) Enns, J. B.; Gillham, J. K. *J. Appl. Polym. Sci.* **1983**, *28*, 2567-2591.
- (38) Surivet, F.; Lam, T. M.; Mai, C.; Pascault, J. P. To be published.
- (39) Martin, J. E.; Adolf, D.; Wilcoxon, J. P. *Phys. Rev.* **1989**, *39*, 1325.